Solidified Liquid Layer Model Expands the Application Fields of Quartz Crystal Microbalance

Long Fu, Yanyan Chen, Hongwei Ma*

The application of a quartz crystal microbalance (QCM) in liquid is hindered by the complexity of data analysis. Recently, a "solidified liquid layer" (SLL) model has been proposed to simplify the data analysis. Here, missing evidence to support the SLL model is provided: 1) the SLL model is responsive to the density change of the liquid environment, 2) thickness values from the SLL model (T_{SLL}) are in agreement with values measured by ellipsometry. The SLL model predicts that a 0.18 nm change of T_{SLL} will lead to a 1 Hz signal, which is the resolution that most commercial QCMs could easily achieve. Using the SLL model, Au–S bond breakage has been successful. Biosensor applications are also being designed according to the SLL model. It is believed that with these results, the SLL model will bring QCM back to the radar screen of scientists.

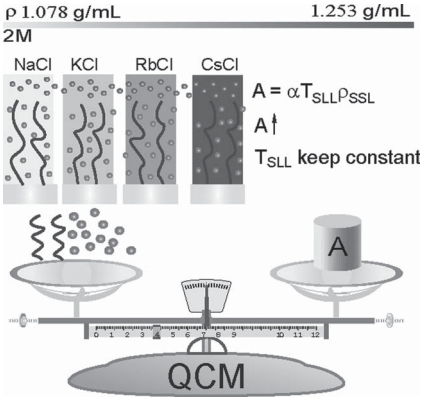

1. Introduction

The quartz crystal microbalance (QCM) is a well-studied instrument, such that some researchers consider it an exhausted mine. Except for routine applications such as monitoring the process of layer-by-layer assembly,[1–3] QCM seems to be insulated from the frontiers of polymer research. On the other hand, compared with surface plasma resonance (SPR), which has achieved great success commercially, QCM is far less popular as a biosensor due to its limited sensitivity[4] as well as difficulties in data interpretation, i.e., it is difficult to indiscriminately separate frequency changes contributed to by mass or viscoelasticity changes when operated in liquid environments.[5–7] A number of theories and instrumental improvements have been developed to treat such viscoelastic complications but only with limited success.[8–11] For all these reasons, QCM is fading away from most researchers' sight. Recently, we proposed a "solidified liquid layer" model (SLL) and successfully applied this SLL model to expand the studied objects of QCM, especially in the polymer related fields. This feature article is written in the hope that this SLL model will bring QCM back to the radar screen of scientists.

The proposed SLL model was based on linear frequency–thickness (F-T) relations revealed over the past six-year period.[5,12] The key that led to the discovery of linear F-T relations was a surface modification strategy, namely surface initiated polymerization (SIP). One simple analogy could make the story short yet crystal clear: one could view SIP for the SLL model as a thermo evaporator for the Sauerbrey equation. When the Sauerbrey equation first predicted a linear F-T relation for ultra-thin metal film coatings on QCM chips under vacuum conditions,[13] proof was needed. It was the thermo evaporator that

Dr. Y. Chen, Dr. H. Ma
Division of Nanobiomedicine, Suzhou Institute of Nano-Tech and Nano-Bionics, Chinese Academy of Sciences, Suzhou, Jiangsu 215123, P. R. China
E-mail: hwma2008@sinano.ac.cn
Mr. L. Fu
Academy for Advanced Interdisciplinary Studies, Peking University, Beijing 100871, P. R. China

Macromol. Rapid Commun. **2012**, *33*, DOI: 10.1002/marc.201100878

allowed the preparation of ultra-thin metal films with the control over the thickness in nanometer steps, which thus made the validation of the linear F-T relation possible. QCM achieved great success as a thickness monitor in the vacuum deposition industry, and was also widely applied in mass and chemical measurement.[14,15] For the SLL model, the story began with the attempts, by Huck's group[16] and us,[17] of applying QCM to monitor in situ the process of SIP. We realized later on that SIP allowed us to prepare surface-tethered polymer coatings under liquid conditions and control the thickness in nanometer steps, which is similar to a thermo evaporator in terms of adding mass to a QCM chip. This ability directly led to the discovery of reported linear F-T relations[5,12] and the build-up of a simple physical model of multi-layer analysis.[5] We were surprised when several linear F-T relations were identified. Yet, it was this surprise that drove us to conduct systematic studies that revealed the underlying mechanisms bit by bit and finally reach this SLL model.

2. Getting Started with QCM

The absolute frequency of a polymer-coated QCM chip in a liquid was determined by two layers[4] (Scheme 1): 1) Layer I has a semi-infinite thickness compared with the penetration depth of an acoustic wave and was characterized by viscosity (η_L) and density (ρ_L), where the subscript L indicates liquid; 2) Layer II was characterized by four parameters, namely elasticity (μ_f), viscosity (η_f), density (ρ_f), and thickness (T_f), where the subscript f indicates a polymeric film.

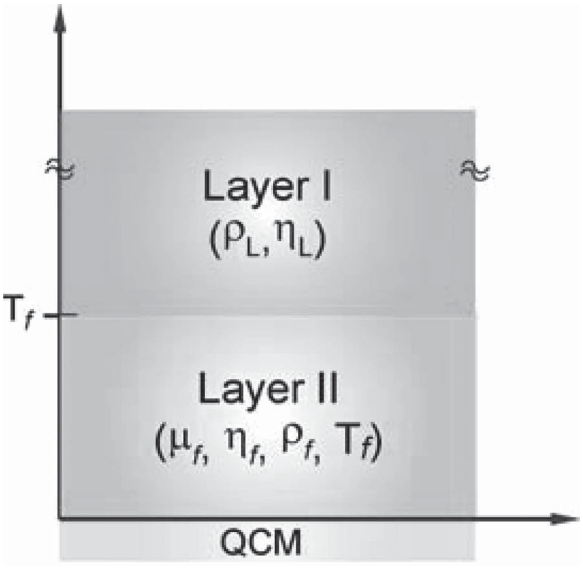

Scheme 1. Physical image of the continuum mechanical model. Layer I was characterized by viscosity (η_L) and density (ρ_L), where the subscript L indicates liquid. Layer II was characterized by four parameters, namely elasticity (μ_f), viscosity (η_f), density (ρ_f) and thickness (T_f), where the subscript f indicates a polymeric film.

Hongwei Ma obtained his Ph.D. in biomedical engineering (BME) under the supervision of Prof. Ashutosh Chilkoti at Duke University (2005). After graduation, he joined Peking University and worked as a principle investigator for three years. Hongwei currently works as a professor of BME at Suzhou Institute of Nano-Technology and Nano-Bionics, Chinese Academy of Sciences (SINANO, CAS). His research interests focus on the application of polymers to solve problems in BME, including the mechanism and application of surface-initiated polymerization, biosensors, protein microarrays, and translational researches.

Long Fu obtained his Bachelor degree in chemistry at Peking University (2007). He is currently a Ph.D. candidate under the supervision of Prof. Hongwei Ma. His thesis focuses on the development and application of the QCM-SLL model.

Yanyan Chen obtained her Ph.D. at Institute of Mechanics, CAS. She currently works as an associate professor of BME at SINANO, CAS. Her research interests focus on biosensors including: mimicking the bio-interface, high sensitivity optical techniques, and the biomedical application of biosensors.

In typical uses of QCM under a liquid environment, information of the following four states are valuable, which are shown in Scheme 2: 1) State 1: a bare chip in air. The absolute vibration frequency of each bare chip in air must be measured and is referred to as the ground zero state; 2) State 2: a bare chip in liquid. One exposes a bare chip to liquid to get a reference value (Δf_n^i *is the overtone number, n = 1, 3, 5, 7…*), which is determined by the density and viscosity of liquid in use (equation 1):

$$\Delta f_n^i \propto (\rho_L \eta_L)^{1/2} \quad (1)$$

This is known as the Kanazawa equation[18] Typically, $\Delta f_3 i/3$ (exposed to water, 25 °C) is 380 Hz. Note, QCM chips used in this article are 5 MHz AT-cut chips. 3) State 3: QCM chip with a coating in air. One measures the frequency change in air/vacuum after the addition of a coating (i.e., the frequency change between state 1 and 3), which is marked as Δf_n^{iii}. While vacuum is not necessary, humidity control is essential to minimize variation. There is a linear *F–T* relation between the frequency change and thickness of coating, which is similar to the Sauerbrey equation,[13] and can be further transformed to Equation (2):

Macromol. Rapid Commun. 2012, DOI: 10.1002/marc.201100878

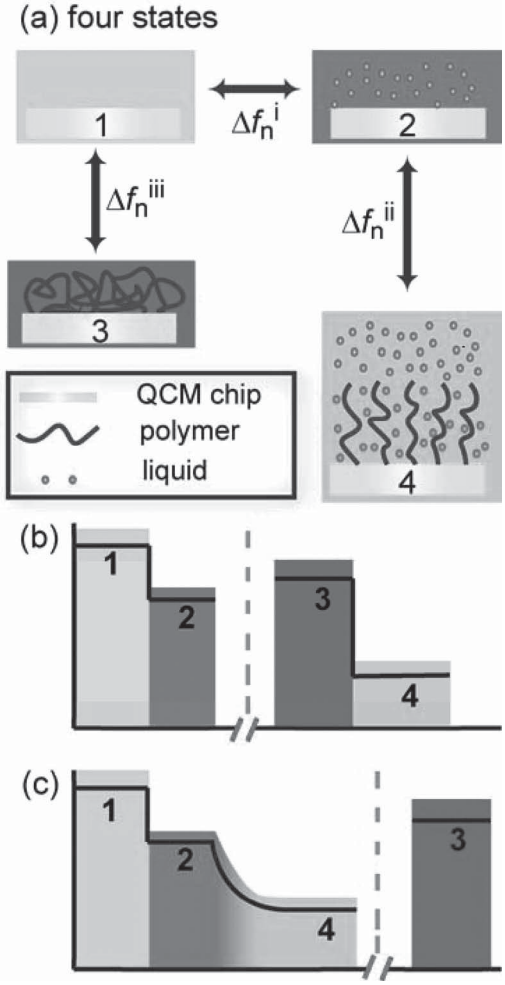

Scheme 2. a) Four states in QCM application are illustrated. 1: bare chip in air; 2: bare chip in a liquid environment; 3: coated chip in air; 4: coated chip in liquid. See text for details of Δf. b,c)The two most common situations for QCM applications.

$$\Delta f_n^{iii}/n = -k\Delta T \quad (2)$$

In Equation (2), ΔT is the thickness of the coated polymer and k is a constant. Most polymers give a k value around 7 with poly(furfuryl methacrylate) (polyFMA) being an exception (k = 13), which is due to its high density as a monomer.[19] In practice, we now use QCM measurement (i.e., Δf_n^{iii}) to replace the needs of ellipsometry in dry states. 4) State 4: QCM chips with a coating in liquid. Here we use a surface tethered polymer chain as a demonstration. Biopolymers, such as DNA and proteins are similarly applicable.[20,21] The frequency change between state 2 and 4 is defined as Δf_n^{ii}, which contains frequency changes contributed by both mass and viscoelasticity changes. We developed a set of equations (Equations (3–5))[22] to separate mass and viscoelasticity induced frequency changes.

$$-\Delta f_n^{ii} = An + Bn \quad (3)$$

$$A = 2f_0^2\rho_f T_f/Z_q \quad (4)$$

$$B = -\,4\pi f_0^2\rho_L T_L J_f/Z_q \quad (5)$$

where n is the overtone number (n = 3,5,7……), A and B are frequency changes caused by wet mass and viscoelasticity, respectively; f_0 = 5 MHz is the fundamental frequency of quartz crystal, and $Z_q = 8.8 \times 10^6$ kg m^{-2} s^{-1} is the acoustic impedance of a quartz crystal.

Scheme 2 also presents two flow-charts that describe the two most common situations for QCM applications: 1) Scheme 2b: state 1 > state 2; state 3 > state 4. Transitions from state 1 to state 2 and from state 3 to state 4 were conducted in a continuous mode, while from state 1 to state 3 was in a discontinuous mode. 2) Scheme 2c: state 1 > state 2 > state 4 was conducted in a continuous mode, while from state 4 to state 3 was in a discontinuous mode. Typical cases are by SIP[23] or biopolymer adsorption to the surface.[20] In the discontinuous mode, the QCM chip has to be unmounted from the sensor, which will lead to frequency variation but this can be minimized and is negligible for most applications.[5] For both situations, state 4 could be events such as pH/thermo changes and ligand–receptor binding, all of which will be reported as frequency changes and be conducted in a continuous mode.[24–30] The challenge then will be how to interpret these frequency changes, even the wet mass information (A in Equation (3)) could be extracted. We will show below that with the SLL model, QCM could be a powerful tool in studying these interfacial events.

3. Validation of the SLL Model

The SLL model focuses on the wet mass, A from Equation (3) (Scheme 3). In the SLL model, surface-tethered polymers act as stakes that solidify liquid, which is similar to the physical model of a coil in solution: a non-free-draining polymer chain behaves as rigid sphere, and the occluded solvent is dragged along with it.[31,32] Equation (5) could be further developed to the following form:

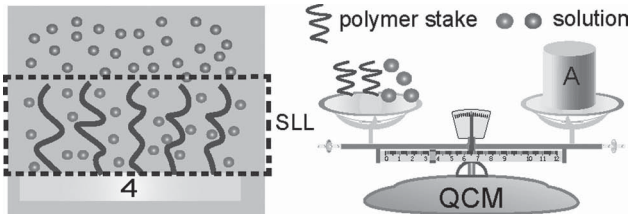

Scheme 3. Illustration of the SLL model. In this model, the mass of QCM sensed includes the mass of stakes and co-vibrating liquid surrounding them. The thickness of the SLL is determined by the swelling state of the surface-tethered polymers.

$$A = \frac{2f_0^2}{Z_q} \times T_{SLL}\rho_{SLL} = \alpha \times T_{SLL}\rho_{SLL} \quad (6)$$

$$\alpha = \frac{2f_0^2}{Z_q} \quad (7)$$

where ρ_{SLL} and T_{SLL} are the density and thickness of SLL, respectively, and α is a constant and is 5.7×10^6 m^2 kg^{-1} s^{-1} for a 5 MHz AT-cut QCM chip. In previous reports we assumed that the SLL has the same density as the solution so that T_{SLL} could be obtained, which made QCM a nice molecular ruler.[4,20,21] Herein, we provide missing pieces of evidence that support the SLL model with surface-tethered polymer chains.

First, we demonstrated that T_{SLL} was consistent with the thickness value measured by ellipsometry. In previously studies,[24,25] we reported that a surface-tethered weak polyelectrolyte film would swell as the concentration of NaCl in solution increased (Figure 1 a), which has been theoretically predicted.[33] Here we prepared two surface-tethered weak polyelectrolyte samples, namely carboxylated poly(2-hydroxyethyl methacrylate) (abbreviated as pHEMA$_{COOH}$) and carboxylated poly(oligo(ethylene glycol) methacrylate-*ran*-2-hydroxyethyl methacrylate) (pOEGMA-*r*-HEMA$_{COOH}$), and applied QCM and ellipsometry to monitor the T_{SLL} change as the [NaCl] increased. Details of sample preparation could be found in previous publications.[25] For the QCM measurements, we assumed the ρ_{SLL} value to be that of the NaCl solution, ρ_{NaCl} = 1.000 g mL^{-1} (measured by a Densito 30PX, METTLER. The density for [NaCl] from 10×10^{-3} to 1 M was determined to be 1.000 to 1.040 g mL^{-1}). The T_{SLL} of polyelectrolytes in NaCl solution were calculated by Equation (6) and shown as the black triangles in Figure 1b and c. The trend that T_{SLL} increased as [NaCl] increased was consistent with previous reports.

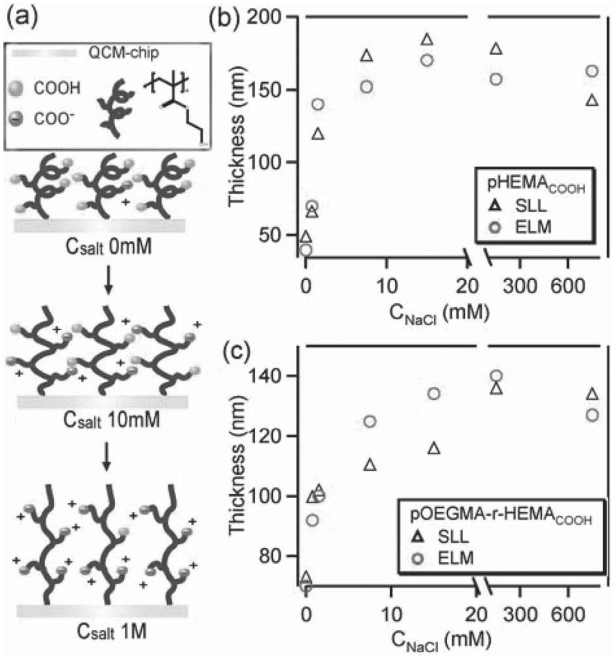

Figure 1. T_{SLL} is consistent with ellipsometry. a)Surface-tethered weak polyelectrolyte swells as [salt] increased. b) pHEMA$_{COOH}$, dry thickness=33.2nm,initiatordensity=2.5%.c)pOEGMA-*r*-HEMA$_{COOH}$ with 1:1 monomer feed ratio, dry thickness = 29.4 nm, initiator density = 2.5%.

Real-time dynamic measurements were performed to obtain the thickness of polymer during the swelling process with a variable angle spectroscopic ellipsometer (Model M2000, J.A. Woollam). The sample was put into a home-made liquid cell. Ellipsometric dynamic data was obtained at an angle of incidence of 75° and a wavelength of 500 nm. A simple four phase model of liquid–Cauchy layer–Au layer (88 nm)–SiO_2 is used to fit the thickness of the polymer, where the Cauchy layer denotes the swelling polymer. The thickness and the refractive index of the swelling polymer are simultaneously fitted with point by point fitting. The ellipsometry results (red circles in Figure 1b and c) demonstrated not only the same trend of swelling but also very similar thickness values, which was strong evidence that the ρ_{SLL} assumption was reasonable.

Second, we demonstrated that the SLL model is responsive to significant ρ_{SLL} change. In this designed experiment, we applied salt solutions with different density, namely 2 M, pH 8.5 MCl (M = Na, K, Rb, Cs, whose density were 1.078, 1.090, 1.170, and 1.253 g mL^{-1}, respectively), to surface-tethered weak polyelectrolytes. Since the metal ions were all monovalent cations, we assumed that the swelling thickness of the polyelectrolytes would remain unchanged. This assumption was supported by ellipsometry measurements: as shown in Figure 2b, ellipsometry results indicated a constant 90 and 80 nm wet thickness of two surface-tethered pOEGMA-*r*-HEMA$_{COOH}$ samples in these four different salt solutions. The same samples were further measured for T_{SLL} by QCM with the same salt solutions. As shown in Figure 2, while the values of A increased linearly as the density increased (i.e., changing solutions from NaCl to CsCl, Figure 2c), T_{SLL} remained constant at 90 and 85 nm, which were not only predicated by Equation (6) but were also very close to the ellipsometry results.

In Equation (6), the mass of SLL can be divided into two parts: polymer stakes ($\Delta m_{polymer}$) and solidified solution (Δm_{sol}). Since $\Delta m_{polymer}$ can be calculated from Δf_n [iii], Δf_{sol} can also be extracted by Equation (9):

$$A = \frac{2f_0^2}{Z_q} \times T_{SLL}\rho_{SLL} = \alpha \times T_{SLL}\rho_{SLL} = \alpha \times \Delta m = \alpha \times (\Delta m_{polymer} + \Delta m_{sol}) \quad (8)$$

$$A - \alpha \times \Delta m_{polymer} = \alpha \times \Delta m_{sol} = \beta \times \rho_{sol} \quad (9)$$

Macromolecular Journals
Macromol. Rapid Commun. **2012**, DOI: 10.1002/marc.201100878

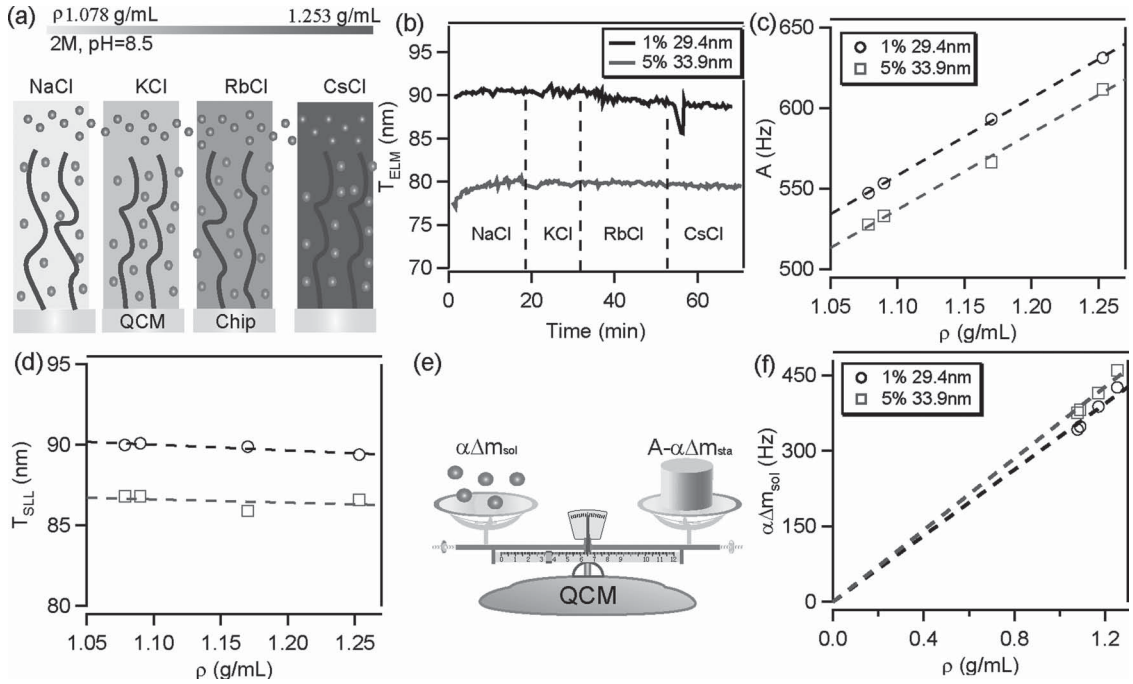

Figure 2. SLL model is responsive to significant ρ_{SLL} change. a) Experimental design for density sensitivity. b) Ellipsometry measurement for wet thickness of surface-tethered polyelectrolytes in different salt solutions. The SLL model responded to the density increase of different salt solutions: c) A value increased linearly as ρ_{salt} increased while d) T_{SLL} remained constant. e)The mass of liquid can also be measured and f) this mass is linearly related to ρ_{salt} with no intercept. Samples used are pOEGMA-*r*-HEMA$_{COOH}$ with a 1:1 feed ratio of monomer, 29.4 nm, 1% initiator density for black circle and 33.9 nm, 5% initiator density for blue square.

where Δm represents the mass of SLL, $\Delta m_{polymer}$ is the mass of the polymer stake and Δm_{sol} is the mass of the solidified liquid, and β is a constant. When plotting Δm_{sol} with ρ_{sol}, one finds a linear relation ($R^2 > 0.9$) and no intercept in the fitted line (Figure 2f).

By now we have presented evidence that 1) T_{SLL} is in agreement with values obtained by ellipsometry, 2) the SLL model is responsive to density change. One thing left unchecked is the density condition under which the SLL could be applied. Bigen et al. theoretically studied how a polymer and its co-vibrating liquid affect the QCM signal. Their results indicated that polymer stakes on the surface might be too dilute to form a uniform layer.[34] Our experimental findings indicate there might also be a high limit of density for the SLL model to be valid. In Figure 2, while T_{SLL} = 90 nm perfectly matched with the ellipsometry thickness for the 1% initiating density sample, there was a 6% difference (85 versus 80 nm) for the 5% initiating density sample. We are currently determining the density range in which SLL is valid.

4. Applications of the SLL Model

In this section, we present applications of the SLL model in different fields, including stem-looped ssDNA de-looping, the thermo response of poly(*N*-isopropyl acrylamide) (pNIPAM), the swelling behaviour of surface-tethered weak polyelectrolytes, and swelling-induced bond breakage. With this SLL model, the QCM signal is transcribed to thickness change rather than mass change.

In electrochemical DNA detection, due to the capability of hybridization-induced conformational change, " stem-loop" ssDNA is an excellent probe for sequence-specific detection of DNA.[35,36] After immobilizing a stem-loop structured ssDNA on a gold-coated QCM chip, one can use a sequence-specific complementary ssDNA to open the loop, and observe a thickness doubling behaviour. By the SLL model, QCM can quantitatively monitor this de-looping process.[21] As shown in Figure 3, when the stem-loop ssDNA is adsorbed on the surface, T_{SLL} was 4.4 nm. After the complementary ssDNA was added to the solution, the T_{SLL} increased to 9.2 nm, which represented the de-looping process.

As a thermo-responsive polymer, pNIPAM has found uses in many applications.[37,38] We applied QCM to study the low critical solution temperature (LCST) behaviour of pNIAPM. Here we re-interpreted the QCM data with the SLL model.[27] As shown in Figure 4 b, the T_{SLL} of pNIPAM decreased as the temperature increased. Around 32 °C, the thickness change was most significant. After 37 °C, the T_{SLL} of pNIPAM was equal to the thickness in its dry

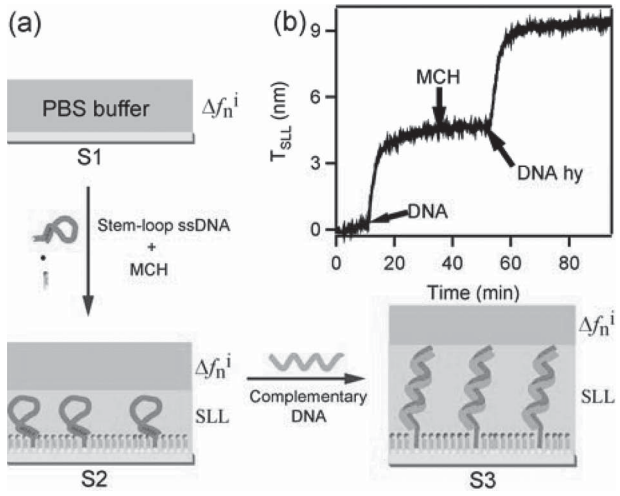

Figure 3. DNA acted as stakes. a) T_{SLL} change due to the immobilization of stem-loop ssDNA (S2) and the hybridization of a complementary strand (S3). b) Real time monitoring of T_{SLL} induced by S2 and S3, A = 95.5 and 185.8 Hz, corresponding to 4.4 and 9.2 nm.

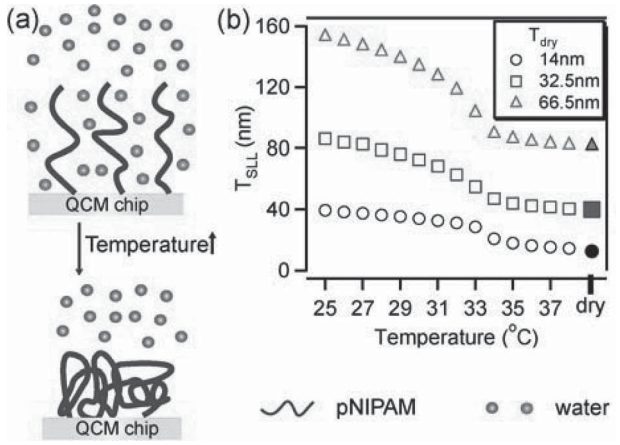

Figure 4. Study of the thermo-responsive behaviour of pNIPAM. a) Experimental design, b) three pNIPAM samples with different thickness were tested, namely black circle, 14 nm; blue square, 32.5 nm; red triangle, 66.5 nm. Solid circle, square, and triangle represent the thickness of the films in a dry state (by ellipsometry).

state, indicating pNIPAM was completely collapsed. This method may find use in the development of new thermo-responsive polymers.[39,40]

A surface-tethered weak polyelectrolyte film was predicted to swell upon the addition of salt solutions even without changing the pH of the solutions.[33] This behaviour was difficult to study but now it is easy with QCM.[24,25] Using the SLL model, one can see this behaviour directly. As shown in Figure 1b, the T_{SLL} of p(OEGMA-*r*-HEMA)$_{COOH}$ continued to increase until $[Na^+] > 10 \times 10^{-3}$ M. Surprisingly, when T_{SLL} was greater than ~250 nm, the Au–S bond was broken (Figure 5b).[25] This direct observation

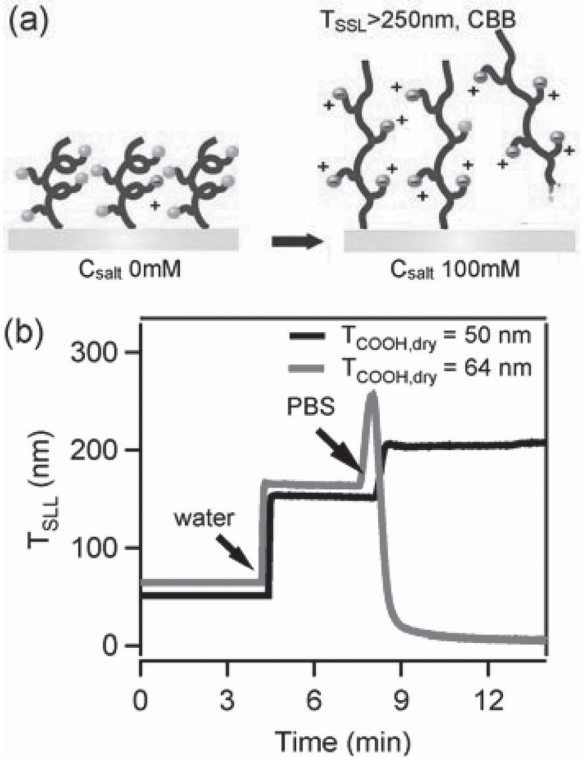

Figure 5. Direct observation of Au–S bond breakage. a) Illustration of the swelling behaviour of a surface-tethered polyelectrolyte in salt solutions. b) Au–S bond breakage was induced at 10×10^{-3} M PBS (pH = 7.4), carboxylated poly(OEGMA-*r*-HEMA) film, with 2.5% initiator density, dry thicknesses were measured by ellipsometry.

of in situ Au–S bond breakage would not be possible otherwise.

5. Conclusions and Outlook

It is not necessary for the SLL model to be superior compared to impedance or dissipation methods. Readers interested in obtaining the viscoelastic information of studied objects should refer to the Q-tools by Q-Sense or free online software (http://www.pc.tu-clausthal.de/forschung/ak-johannsmann/qcm-modellierung/). In fact, the SLL model was not designed to tackle the viscoelastic complication. Instead, the SLL model was designed to make a detour, to simplify data interpretation for QCM in liquid. So QCM data (frequency change) could be interpreted by chemists (especially in the field of polymer science) and biologists, who might not be interested in dealing with mathematics.

We are confident that the SLL model is not one model too many. For example, what Lineweaver and Burk did in the most cited JACS paper[41] was to transform a known Equation (10) (also known as the Michaelis–Menten equation) to Equation (11),

$$V_0 = V_{max} \frac{[S]}{K_M + [S]} \quad (10)$$

$$\frac{1}{\upsilon} = \frac{K_M}{V_{max}[S]} + \frac{1}{V_{max}} \quad (11)$$

With this simple transformation, the experimental results can be linearly plotted and V_{max} and K_m can be easily calculated. Back to the SLL model, it reveals for the first time that a 0.18 nm thickness change of SLL leads to a 1 Hz signal, which makes QCM a highly sensitive instrument for sensing thickness change under a liquid environment. Thus, we believe this SLL model is also a useful transformation that can benefit the QCM users for both understanding how QCM works and expanding the application fields of QCM.

Acknowledgements; This work was supported by the 100 Talents Program of CAS (08BM031001), National Basic Research Program of China (2009CB320300), and NSFC (21074148, 21174161) to H.M. The authors thank Dr. Chi Wu for suggestions on the non-free-draining theory and Dr. Gang Jin at the Key Laboratory of Microgravity, Institute of Mechanics, CAS for ellipsometry measurements.

Received: December 24, 2011; Revised: February 22, 2012; Published online: ; DOI: 10.1002/marc.201100878

Keywords: quartz crystal microbalance, polyelectrolyte, solidified liquid layer, interface, biosensor

[1] N. Fukao, K.-H. Kyung, K. Fujimoto, S. Shiratori, *Macromolecules* **2011**, *44*, 2964.
[2] T. Serizawa, K. Hamada, T. Kitayama, N. Fujimoto, K. Hatada, M. Akashi, *J. Am. Chem. Soc.* **2000**, *122*, 1891.
[3] T. Serizawa, S. Kamimura, N. Kawanishi, M. Akashi, *Langmuir* **2002**, *18*, 8381.
[4] J. He, Y. Lu, J. Fang, H. Ma, *Sci. China, Ser. B* **2011**, DOI: 10.1007/s11426-011-4467-8.
[5] L. Fu, X. Chen, J. He, C. Xiong, H. Ma, *Langmuir* **2008**, *24*, 6100.
[6] M. D. Ward, D. A. Buttry, *Science* **1990**, *249*, 1000.
[7] C. C. White, J. L. Schrag, *J. Chem. Phys.* **1999**, *111*, 11192.
[8] D. Johannsmann, K. Mathauer, G. Wegner, W. Knoll, *Phys. Rev. B* **1992**, *46*, 7808.
[9] A. Jörg, H. Peter, H. Jens, R. Steffen, L. Ralf, *Sensor. Actuat. B-Chem.* **1995**, *24*, 43.
[10] M. V. Voinova, M. Jonson, B. Kasemo, *Biosens. Bioelectron.* **2002**, *17*, 835.
[11] M. V. Voinova, M. Rodahl, M. Jonson, B. Kasemo, *Phy. Scr.* **1999**, *59*, 391.
[12] J. He, Y. Wu, J. Wu, X. Mao, L. Fu, T. Qian, J. Fang, C. Xiong, J. Xie, H. Ma, *Macromolecules* **2007**, *40*, 3090.
[13] G. Sauerbrey, *Zeitschrift Fur Physik* **1959**, *155*, 206.
[14] G. G. Guilbault, J. M. Jordan, *Crit. Rev. Anal. Chem.* **1988**, *19*, 1.
[15] J. F. Alder, J. J. McCallum, *Analyst* **1983**, *108*, 1169.
[16] S. E. Moya, A. A. Brown, O. Azzaroni, W. T. S. Huck, *Macromol. Rapid Commun.* **2005**, *26*, 1117.
[17] H. Ma, M. Textor, R. L. Clark, A. Chilkoti, *Biointerphases* **2006**, *1*, 35.
[18] K. K. Kanazawa, J. G. Gordon, *Anal. Chem.* **1985**, *57*, 1770.
[19] J. He, L. Fu, M. Huang, Y. Lu, B. e. Lv, Z. Zhu, J. Fang, H. Ma, *Sci. China, Ser. B* **2011**, *41*, 1679.
[20] M. Huang, J. a. He, J. Gan, H. Ma, *Colloids Surf., B* **2011**, *85*, 92.
[21] H. Ma, J. a. He, Z. Zhu, B. e. Lv, D. Li, C. Fan, J. Fang, *Chem. Commun.* **2010**, *46*, 949.
[22] Y. Zhang, B. Du, X. Chen, H. Ma, *Anal. Chem.* **2009**, *81*, 642.
[23] X. Chen, Y. Zhang, J. He, C. Xiong, Y. Meng, G. Jin, H. Ma, *Sci. China, Ser. B* **2009**, *52*, 2307.
[24] Y. Zhang, J. a. He, Y. Zhu, H. Chen, H. Ma, *Chem. Commun.* **2011**, 1190.
[25] Y. Zhang, B. e. Lv, Z. Lu, J. a. He, S. Zhang, H. Chen, H. Ma, *Soft Matter* **2011**, *7*, 11496.
[26] N. Schuewer, H.-A. Klok, *Langmuir* **2011**, *27*, 4789.
[27] H. Ma, L. Fu, W. Li, Y. Zhang, M. Li, *Chem. Commun.* **2009**, 3428.
[28] G. M. Liu, G. Z. Zhang, *J. Phys. Chem. B* **2005**, *109*, 743.
[29] Y. Liu, X. Yu, R. Zhao, D. H. Shangguan, Z. Y. Bo, G. Q. Liu, *Biosens. Bioelectron.* **2003**, *19*, 9.
[30] M. Muratsugu, F. Ohta, Y. Miya, T. Hosokawa, S. Kurosawa, N. Kamo, H. Ikeda, *Anal. Chem.* **1993**, *65*, 2933.
[31] H. Yamakawa, *Modern Theory of Polymer Solutions*, Harper & Row, New York **1971**.
[32] R. Larson, *Constitutive Equations for Polymer Melts and Solutions,* Butterworth-Heinemann, Boston **1988**.
[33] E. B. Zhulina, T. M. Birshtein, O. V. Borisov, *Macromolecules* **1995**, *28*, 1491.
[34] P. Bingen, G. Wang, N. F. Steinmetz, M. Rodahl, R. P. Richter, *Anal. Chem.* **2008**, *80*, 8880.
[35] C. H. Fan, K. W. Plaxco, A. J. Heeger, *Proc. Natl. Acad. Sci. U.S.A.* **2003**, *100*, 9134.
[36] G. Liu, Y. Wan, V. Gau, J. Zhang, L. Wang, S. Song, C. Fan, *J. Am. Chem. Soc.* **2008**, *130*, 6820.
[37] H. G. Schild, *Prog. Polym. Sci.* **1992**, *17*, 163.
[38] S. K. Ahn, R. M. Kasi, S. C. Kim, N. Sharma, Y. X. Zhou, *Soft Matter* **2008**, *4*, 1151.
[39] J. F. Lutz, A. Hoth, *Macromolecules* **2006**, *39*, 893.
[40] J.-F. Lutz, O. Akdemir, A. Hoth, *J. Am. Chem. Soc.* **2006**, *128*, 13046.
[41] H. Lineweaver, D. Burk, *J. Am. Chem. Soc.* **1934**, *56*, 658.